Supplement of Atmos. Chem. Phys., 21, 7611–7638, 2021
https://doi.org/10.5194/acp-21-7611-2021-supplement

Atmospheric Chemistry and Physics
Open Access
EGU

Supplement of

Time-dependent 3D simulations of tropospheric ozone depletion events in the Arctic spring using the Weather Research and Forecasting model coupled with Chemistry (WRF-Chem)

Maximilian Herrmann et al.

Correspondence to: Maximilian Herrmann (maximilian.herrmann@iwr.uni-heidelberg.de)

S1 Chemistry mechanism extensions

S1.1 Gas phase halogen reactions added to the MOZART-4 mechanism

Table S1: Additional gas phase halogen reactions

# Reac.	Reaction	$k\left[\left(\text{molec.}\,\text{cm}^{-3}\right)^{1-n}\text{s}^{-1}\right]$	Reference
1	$O_3 + Br \rightarrow O_2 + BrO$	$1.7 \times 10^{-11} \exp(-800/T)$	Atkinson et al. (2007)
2	$2BrO \rightarrow 2Br + O_2$	2.7×10^{-12}	Atkinson et al. (2007)
3	$2BrO \rightarrow Br_2 + O_2$	$2.9 \times 10^{-14} \exp(840/T)$	Atkinson et al. (2007)
4	$BrO + HO_2 \rightarrow HOBr + O_2$	$4.5 \times 10^{-12} \exp(500/T)$	Atkinson et al. (2007)
5	$Br + HO_2 \rightarrow HBr + O_2$	$7.7 \times 10^{-12} \exp(-450/T)$	Atkinson et al. (2007)
6	$Br + CH_2O \xrightarrow{O_2} HBr + CO + HO_2$	$7.7 \times 10^{-12} \exp(-580/T)$	Atkinson et al. (2007)
7	$Br + C_2H_2 \xrightarrow{3O_2} Br + 2CO + 2HO_2$	4.2×10^{-14}	Borken (1996)
8	$Br + C_2H_2 \xrightarrow{2O_2} HBr + 2CO + HO_2$	8.92×10^{-14}	Borken (1996)
9	$Br + C_2H_4O \xrightarrow{O_2} HBr + CH_3CO_3$	$1.8 \times 10^{-11} \exp(-460/T)$	Atkinson et al. (2007)
10	$Br_2 + OH \rightarrow HOBr + Br$	$2.0 \times 10^{-11} \exp(240/T)$	Atkinson et al. (2007)
11	$HBr + OH \rightarrow Br + H_2O$	$6.7 \times 10^{-12} \exp(155/T)$	Atkinson et al. (2007)
12	$Br + C_2H_4 \xrightarrow{3.5O_2} Br + 2CO + H_2O + 2HO_2$	2.53×10^{-13}	Barnes et al. (1993)
13	$Br + C_2H_4 \xrightarrow{2.5O_2} HBr + 2CO + H_2O + HO_2$	5.34×10^{-13}	Barnes et al. (1993)
14	$BrO + CH_3O_2 \rightarrow HOBr + OH + HO_2 + CO$	$2.4 \times 10^{-14} \exp(1617/T)$	Atkinson et al. (2007)
15	$HOBr + O(^3P) \rightarrow BrO + O_2$	$1.2 \times 10^{-10} \exp(-430/T)$	Nesbitt et al. (1995)
16	$NO_3 + Br \rightarrow NO_2 + BrO$	1.6×10^{-11}	Atkinson et al. (2007)
17	$NO_2 + BrO + M \rightarrow BrONO_2 + M$	$k_0 = 4.7 \times 10^{-31}(T/300)^{-3.1}\,[N_2]$ $k_\infty = 1.8 \times 10^{-11}$ $F_c = 0.4$	Atkinson et al. (2007)
18	$NO + BrO \rightarrow NO_2 + Br$	$8.7 \times 10^{-12} \exp(260/T)$	Atkinson et al. (2007)
19	$HOCl + O(^3P) \rightarrow ClO + OH$	1.7×10^{-13}	Atkinson et al. (2007)
20	$ClO + O(^3P) \rightarrow Cl + O_2$	$2.5 \times 10^{-11} \exp(110/T)$	Atkinson et al. (2007)
21	$OClO + O(^3P) \rightarrow ClO + O_2$	$2.4 \times 10^{-12} \exp(-960/T)$	Atkinson et al. (2007)
22	$ClONO_2 + O(^3P) \rightarrow 0.5ClO$ $+0.5NO_3 + 0.5OClO + 0.5NO_2$	$4.5 \times 10^{-12} \exp(-900/T)$	Atkinson et al. (2007)
23	$Cl + HO_2 \rightarrow HCl + O_2$	3.4×10^{-11}	Atkinson et al. (2007)
24	$Cl + HO_2 \rightarrow ClO + OH$	$6.3 \times 10^{-11} \exp(-570/T)$	Atkinson et al. (2007)
25	$Cl + H_2O_2 \rightarrow HCl + HO_2$	$1.1 \times 10^{-11} \exp(-980/T)$	Atkinson et al. (2007)
26	$Cl + O_3 \rightarrow ClO + O_2$	$2.8 \times 10^{-11} \exp(-250/T)$	Atkinson et al. (2007)
27	$Cl + HNO_3 \rightarrow HCl + NO_3$	2.0×10^{-16}	Atkinson et al. (2007)
28	$Cl + NO_3 \rightarrow ClO + NO_2$	2.4×10^{-11}	Atkinson et al. (2007)
29	$Cl + OClO \rightarrow 2ClO$	$3.2 \times 10^{-11} \exp(170/T)$	DeMore et al. (1997)
30	$Cl + ClONO_2 \rightarrow Cl_2 + NO_3$	$6.2 \times 10^{-12} \exp(145/T)$	Atkinson et al. (2007)
31	$Cl_2 + OH \rightarrow Cl + HOCl$	$3.6 \times 10^{-12} \exp(-1,200/T)$	Atkinson et al. (2007)
32	$HCl + OH \rightarrow Cl + H_2O$	$1.7 \times 10^{-12} \exp(-230/T)$	Atkinson et al. (2007)
33	$HOCl + OH \rightarrow ClO + H_2O$	5.0×10^{-13}	Atkinson et al. (2007)
34	$ClO + OH \rightarrow 0.94Cl$ $+0.94HO_2 + 0.06HCl + 0.06O_2$	$7.3 \times 10^{-12} \exp(300/T)$	Atkinson et al. (2007)
35	$OClO + OH \rightarrow HOCl + O_2$	$1.4 \times 10^{-12} \exp(600/T)$	Atkinson et al. (2007)

# Reac.	Reaction	$k\left[\left(\text{molec.cm}^{-3}\right)^{1-n}\text{s}^{-1}\right]$	Reference
36	$\text{ClONO}_2 + \text{OH} \rightarrow \text{HOCl} + \text{NO}_3$	$1.2 \times 10^{-12} \exp\left(-330/T\right)$	Atkinson et al. (2007)
37	$\text{HCl} + \text{NO}_3 \rightarrow \text{Cl} + \text{HNO}_3$	5.0×10^{-17}	Atkinson et al. (2007)
38	$\text{ClO} + \text{HO}_2 \rightarrow \text{HOCl} + \text{O}_2$	$2.2 \times 10^{-12} \exp\left(340/T\right)$	Atkinson et al. (2007)
39	$\text{ClO} + \text{O}_3 \rightarrow 0.06\text{OClO} + 0.96\text{OClO} + \text{O}_2$	1.6×10^{-17}	Atkinson et al. (2007)
40	$\text{ClO} + \text{NO} \rightarrow \text{Cl} + \text{NO}_2$	$6.2 \times 10^{-12} \exp\left(295/T\right)$	Atkinson et al. (2007)
41	$\text{ClO} + \text{NO}_2 + \text{M} \rightarrow \text{ClONO}_2 + \text{M}$	$k_0 = 1.6 \times 10^{-31}(T/300)^{-3.4}\left[\text{N}_2\right]$ $k_\infty = 7.0 \times 10^{-11}$ $F_c = 0.4$	Atkinson et al. (2007)
42	$\text{ClO} + \text{NO}_3 \rightarrow$ $0.74\text{ClOO} + 0.26\text{OClO} + \text{NO}_2$	4.6×10^{-13}	Atkinson et al. (2007)
43	$2\text{ClO} \rightarrow \text{Cl}_2 + \text{O}_2$	$10^{-12} \exp\left(-1,590/T\right)$	Atkinson et al. (2007)
44	$2\text{ClO} \rightarrow \text{Cl} + \text{ClOO}$	$3.0 \times 10^{-11} \exp\left(-2,450/T\right)$	Atkinson et al. (2007)
45	$2\text{ClO} \rightarrow \text{Cl} + \text{OClO}$	$3.5 \times 10^{-13} \exp\left(-1,370/T\right)$	Atkinson et al. (2007)
46	$2\text{ClO} + \text{M} \rightarrow \text{Cl}_2\text{O}_2 + \text{M}$	$k_0 = 2.0 \times 10^{-32}(T/300)^{-4.0}\left[\text{N}_2\right]$ $k_\infty = 10^{-11}$ $F_c = 0.45$	Atkinson et al. (2007)
47	$\text{Cl}_2\text{O}_2 + \text{M} \rightarrow 2\text{ClO} + \text{M}$	$k_0 = 3.7 \times 10^{-7} \times \exp\left(-7,690/T\right)\left[\text{N}_2\right]$ $k_\infty = 7.9 \times 10^{15} \exp\left(-8,820/T\right)$ $F_c = 0.45$	Atkinson et al. (2007)
48	$\text{OClO} + \text{NO} \rightarrow \text{ClO} + \text{NO}_2$	$1.1 \times 10^{-13} \exp\left(350/T\right)$	Atkinson et al. (2007)
49	$\text{OClO} + \text{Br} \rightarrow \text{ClO} + \text{BrO}$	$2.7 \times 10^{-11} \exp\left(-1,300/T\right)$	Atkinson et al. (2007)
50	$\text{Cl}_2\text{O}_2 + \text{Br} \rightarrow \text{BrCl} + \text{ClOO}$	$5.9 \times 10^{-12} \exp\left(-170/T\right)$	Atkinson et al. (2007)
51	$\text{BrO} + \text{ClO} \rightarrow \text{Br} + \text{OClO}$	$1.6 \times 10^{-12} \exp\left(430/T\right)$	Atkinson et al. (2007)
52	$\text{BrO} + \text{ClO} \rightarrow \text{Br} + \text{ClOO}$	$2.9 \times 10^{-12} \exp\left(220/T\right)$	Atkinson et al. (2007)
53	$\text{BrO} + \text{ClO} \rightarrow \text{BrCl} + \text{O}_2$	$5.8 \times 10^{-13} \exp\left(170/T\right)$	Atkinson et al. (2007)
54	$\text{BrCl} + \text{Cl} \rightarrow \text{Br} + \text{Cl}_2$	1.45×10^{-11}	Sander et al. (1997)
55	$\text{Br}_2 + \text{Cl} \rightarrow \text{Br} + \text{BrCl}$	$2.3 \times 10^{-10} \exp\left(135/T\right)$	Sander et al. (1997)
56	$\text{Br} + \text{BrCl} \rightarrow \text{Br}_2 + \text{Cl}$	3.3×10^{-15}	Sander et al. (1997)
57	$\text{Br} + \text{Cl}_2 \rightarrow \text{BrCl} + \text{Cl}$	1.1×10^{-15}	Sander et al. (1997)
58	$\text{Cl} + \text{CH}_4 \xrightarrow{\text{O}_2} \text{HCl} + \text{CH}_3\text{O}_2$	6.6×10^{-12}	Atkinson et al. (2006)
59	$\text{Cl} + \text{C}_2\text{H}_6 \rightarrow \text{HCl} + \text{C}_2\text{H}_5$	$8.3 \times 10^{-11} \exp\left(-100/T\right)$	Atkinson et al. (2006)
60	$\text{Cl} + \text{C}_3\text{H}_8 \xrightarrow{2.5\text{O}_2}$ $\text{HCl} + \text{C}_2\text{H}_5\text{O}_2 + \text{H}_2\text{O} + \text{CO}_2$	1.4×10^{-10}	Atkinson et al. (2006)
61	$\text{Cl} + \text{CH}_2\text{O} \xrightarrow{\text{O}_2} \text{HCl} + \text{CO} + \text{HO}_2$	$8.1 \times 10^{-11} \exp\left(-34/T\right)$	Atkinson et al. (2006)
62	$\text{Cl} + \text{C}_2\text{H}_4\text{O} \xrightarrow{\text{O}_2} \text{HCl} + \text{CH}_3\text{CO}_3$	8.0×10^{-11}	Atkinson et al. (2006)
63	$\text{Cl} + \text{CH}_3\text{O}_2\text{H} \rightarrow \text{HCl} + \text{C}_2\text{H}_4\text{O} + \text{OH}$	5.9×10^{-11}	Atkinson et al. (2006)
64	$\text{Cl} + \text{C}_2\text{H}_5\text{O}_2\text{H} \rightarrow \text{HCl} + \text{C}_2\text{H}_5\text{O}_2$	5.7×10^{-11}	Atkinson et al. (2006)
65	$\text{Cl} + \text{C}_2\text{H}_2 \xrightarrow{3\text{O}_2} \text{Cl} + 2\text{CO} + 2\text{HO}_2$	2.0×10^{-11}	Borken (1996)
66	$\text{Cl} + \text{C}_2\text{H}_2 \xrightarrow{2\text{O}_2} \text{HCl} + 2\text{CO} + \text{HO}_2$	4.24×10^{-11}	Borken (1996)
67	$\text{Cl} + \text{C}_2\text{H}_4 \xrightarrow{3.5\text{O}_2} \text{Cl} + 2\text{CO} + \text{H}_2\text{O} + 2\text{HO}_2$	$k_0 = 1.26 \times 10^{-29} \times (T/300)^{-3.3}\left[\text{N}_2\right]$ $k_\infty = 6.0 \times 10^{-10}$ $F_c = 0.4$	Atkinson et al. (2006)
68	$\text{Cl} + \text{C}_2\text{H}_4 \xrightarrow{2.5\text{O}_2} \text{HCl} + 2\text{CO} + \text{H}_2\text{O} + \text{HO}_2$	$k_0 = 5.92 \times 10^{-30} \times (T/300)^{-3.3}\left[\text{N}_2\right]$ $k_\infty = 6.0 \times 10^{-10}$ $F_c = 0.4$	Atkinson et al. (2006)

# Reac.	Reaction	$k\left[\left(\mathrm{molec.\,cm^{-3}}\right)^{1-n}\mathrm{s^{-1}}\right]$	Reference
69	$\mathrm{Cl + O_2 + M \rightarrow ClOO + M}$	$1.4\times10^{-33}\,(T/300)^{-3.9}\,[\mathrm{N_2}]$ $+1.6\times10^{-33}\,(T/300)^{-2.9}\,[\mathrm{O_2}]$	Atkinson et al. (2007)
70	$\mathrm{ClOO + M \rightarrow Cl + O_2 + M}$	$2.8\times10^{-10}\exp\left(-1,820/T\right)[\mathrm{N_2}]$	Atkinson et al. (2007)
71	$\mathrm{Cl + ClOO \rightarrow 0.95Cl_2 + 0.95O_2 + 0.1ClO}$	2.42×10^{-10}	DeMore et al. (1997)
72	$\mathrm{ClO + CH_3O_2 \rightarrow Cl + CH_2O + HO_2}$	$1.8\times10^{-12}\exp\left(-600/T\right)$	Atkinson et al. (2006)
73	$\mathrm{HBr_m(aq) + HOBr_m(aq) \rightarrow Br_2(g)}$	$1.6\times10^{-5}\,\mathrm{l\,mol^{-1}\,s^{-1}}$	Sander and Crutzen (1996)

Gas-phase reactions are shown in Tab. S1 where reaction rates of three-body reactions are calculated with the Lindemann-Hinshelwood expression (Troe, 1979)

$$k = \frac{k_0}{1+k_0/k_\infty} F_c^{\frac{1}{1+\log(k_0/k_\infty)^2}}. \tag{S1}$$

S1.2 Additional photolysis reactions

Table S2. Additional photolysis reactions. Also given is the corresponding New TUV photolysis rate variable (Madronich et al., 2002)

Reaction	Photolysis rate variable
$\mathrm{Br_2 \rightarrow 2Br}$	j(Pj_br2)
$\mathrm{BrO \rightarrow Br + O}$	j(Pj_bro)
$\mathrm{HOBr \rightarrow Br + OH}$	j(Pj_hobr)
$\mathrm{BrNO_2 \rightarrow Br + NO_2}$	j(Pj_brno2)
$\mathrm{BrONO_2 \rightarrow 0.85Br + 0.85NO_3 + 0.15BrO + 0.15NO_2}$	j(Pj_brono2_a) + j(Pj_brono2_b)
$\mathrm{BrCl \rightarrow Br + Cl}$	j(Pj_brcl)
$\mathrm{Cl_2 \rightarrow 2Cl}$	j(Pj_cl2)
$\mathrm{HOCl \rightarrow Cl + OH}$	j(Pj_hocl)
$\mathrm{ClO \rightarrow Cl + O}$	j(Pj_clo)
$\mathrm{ClONO_2 \rightarrow 0.85Cl + 0.85NO_3 + 0.15ClO + 0.15NO_2}$	j(Pj_clono2_a) + j(Pj_clono2_b)
$\mathrm{OClO \rightarrow ClO + O}$	j(Pj_oclo)
$\mathrm{ClOO \rightarrow ClO + O}$	j(Pj_cloo)
$\mathrm{CHBr_3 \xrightarrow{O_2} 2Br + HBr + CO_2}$	j(Pj_chbr3)
$\mathrm{HCOBr \rightarrow Br + HO_2 + CO}$	3.55×10^{-4} j(Pj_no2)
$\mathrm{CBr_2O \rightarrow 2Br + CO}$	5.66×10^{-5} j(Pj_no2)

Photolysis reactions are detailed in Tab. S2. HCOBr and $\mathrm{CBr_2O}$ are not implemented in the New TUV mechanism and are instead scaled with the $\mathrm{NO_2}$ photolysis rate. The scaling factor is taken as the ratios of 24 h average photolysis rates of $\mathrm{HCOBr/NO_2}$ and $\mathrm{CHr_2O/NO_2}$, respectively, reported by Toyota et al. (2014).

S1.3 Additional depositions and emissions

For ozone, the Wesely dry deposition scheme (Wesely, 1989) for the surface resistance R_{sfc} already implemented in WRF-Chem is used. The other species listed in Tab. S3 have their surface resistance overwritten with the formula (Herrmann et al., 2019)

$$R_{\mathrm{sfc}} = \frac{4}{v_{\mathrm{th}}\delta}, \tag{S2}$$

Table S3. Heterogenous reactions and dry depositions occurring on the snow surface

Reaction/Dry deposition	Accommodation coefficient δ [−]
$\mathrm{HBr} \rightarrow$	0.06
$\mathrm{HOBr} \rightarrow a\ \mathrm{Br_2} + b\ \mathrm{BrCl}$	0.06
$\mathrm{HCl} \rightarrow$	0.06
$\mathrm{BrONO_2} \rightarrow \mathrm{HOBr} + \mathrm{HNO_3}$	0.06
$\mathrm{N_2O_5} \rightarrow \mathrm{BrNO_2} + \mathrm{HNO_3}$	0.09
$\mathrm{O_3} \rightarrow \alpha \mathrm{Br_2}$	-

where v_{th} is the thermal velocity. As described in section 2.4, emission probabilities of Br_2 and BrCl due to HOBr deposition depend on the type of surface and deposition rate of HBr and its aerosol forms. The emission probability of Br_2 due to HOBr deposition is:

$$a = \begin{cases} 1 & \text{on FY ice} \\ \min\left(1, \dfrac{F_{\mathrm{d}}(\mathrm{HBr}) + \sum_{m=1}^{4} F_{\mathrm{d}}(\mathrm{HBr}_m(\mathrm{aq}))}{F_{\mathrm{d}}(\mathrm{HOBr})}\right) & \text{on MY ice or snow} \end{cases} \tag{S3}$$

with $0 \leq a \leq 1$ and $F_{\mathrm{d}} \geq 0$. The emission probability of BrCl due to HOBr deposition is given by

$$b = \begin{cases} 0 & \text{on FY ice or snow} \\ 1 - a & \text{on MY ice} \end{cases} \tag{S4}$$

S1.4 Additional reactions on aerosols

Table S4. Additional reactions on aerosols

Transfer reaction	Molar mass [g]	Molar volume $\left[\mathrm{l mol^{-1}}\right]$	γ [−]	T_γ [K]
$\mathrm{HBr(g)} \rightarrow \mathrm{HBr}_m\mathrm{(aq)}$	80.91	30	0.03	3940
$\mathrm{HOBr(g)} \rightarrow \mathrm{HOBr}_m\mathrm{(aq)}$	96.911	39.2	0.5	0
$\mathrm{BrONO_2(g)} \rightarrow \mathrm{HOBr}_m\mathrm{(aq)} + \mathrm{HNO_3(g)}$	141.01	60.9	0.063	0

The temperature dependence of the accommodation coefficients shown in Tab. S4 is given by

$$\gamma(T) = \left\{1 + (1/\gamma(T_0) - 1)\exp\left[-T_\gamma\left(\frac{1}{T} - \frac{1}{T_0}\right)\right]\right\}^{-1}, \tag{S5}$$

where $T_0 = 298.15$ K.

S2 Vertical distribution of grid cells

Table S5 shows the vertical distribution of grid cells in the present model for a grid cell over sea ice in the center of the domain. WRF-Chem uses an η coordinate, which is an idealized hydrostatic pressure profile mapped to values between zero and unity. Unity corresponds to the ground level and zero to around 50 hPa or 20 km height. It should be noted that the height shown in the table is only an approximate value, since height is temperature dependent due to η being the actual vertical coordinate used by WRF-Chem.

S3 In-situ measurements at Utqiaġvik

Figure S1 shows ozone mixing ratios at Utqiaġvik for simulations 1, 2, 3, 4, and 6 in comparison with in-situ observations.

Table S5. Grid cell number and corresponding η at the lower boundary of the cell as well as pressure and height at the center of the grid cell.

Grid cell number	η [-]	pressure [hPa]	height [m]
1	1.000	99.810	14
2	0.996	99.430	41
3	0.992	99.050	68
4	0.988	98.670	96
5	0.984	98.290	124
6	0.980	97.910	152
7	0.976	97.530	181
8	0.972	97.150	209
9	0.968	96.770	238
10	0.964	96.390	267
11	0.960	95.962	299
12	0.955	95.487	336
13	0.950	95.012	372
14	0.945	94.537	409
15	0.940	94.015	450
16	0.934	93.445	495
17	0.928	92.874	540
18	0.922	92.257	589
19	0.915	91.592	643
20	0.908	90.927	697
21	0.901	90.215	755
22	0.893	89.455	818
23	0.885	88.647	885
24	0.876	87.792	957
25	0.867	86.890	1,033
26	0.857	85.940	1,114
27	0.847	84.942	1,201
28	0.836	83.850	1,296
29	0.824	82.662	1,401
39	0.811	81.380	1,516
31	0.797	79.955	1,646
32	0.781	78.340	1,796

Grid cell number	η [-]	pressure [Pa]	height [m]
33	0.763	76.535	1,967
34	0.743	74.445	2,169
35	0.719	71.975	2,415
36	0.691	69.220	2,698
37	0.661	65.800	3,064
38	0.619	61.192	3,585
39	0.564	56.110	4,199
40	0.512	51.360	4,818
41	0.464	46.990	5,430
42	0.420	42.905	6,044
43	0.378	39.057	6,668
44	0.339	35.495	7,291
45	0.303	32.170	7,923
46	0.269	29.082	8,566
47	0.238	26.280	9,210
48	0.210	23.762	9,854
49	0.185	21.482	10,507
50	0.162	19.440	11,159
51	0.142	17.587	11,816
52	0.123	15.877	12,488
53	0.106	14.357	13,149
54	0.091	12.980	13,813
55	0.077	11.745	14,469
56	0.065	10.605	15,140
57	0.053	9.560	15,819
58	0.043	8.657	16,468
59	0.034	7.850	17,109
60	0.026	7.090	17,778
61	0.018	6.425	18,421
62	0.012	5.855	19,031
63	0.006	5.285	19,704

S4 Tropospheric BrO VCDs for simulations 4 and 6

In this section, the BrO VCDs for simulations 1-4 and 6, following Figs. 10 and 11 in the main text, are shown in Figs. S2 and S3.

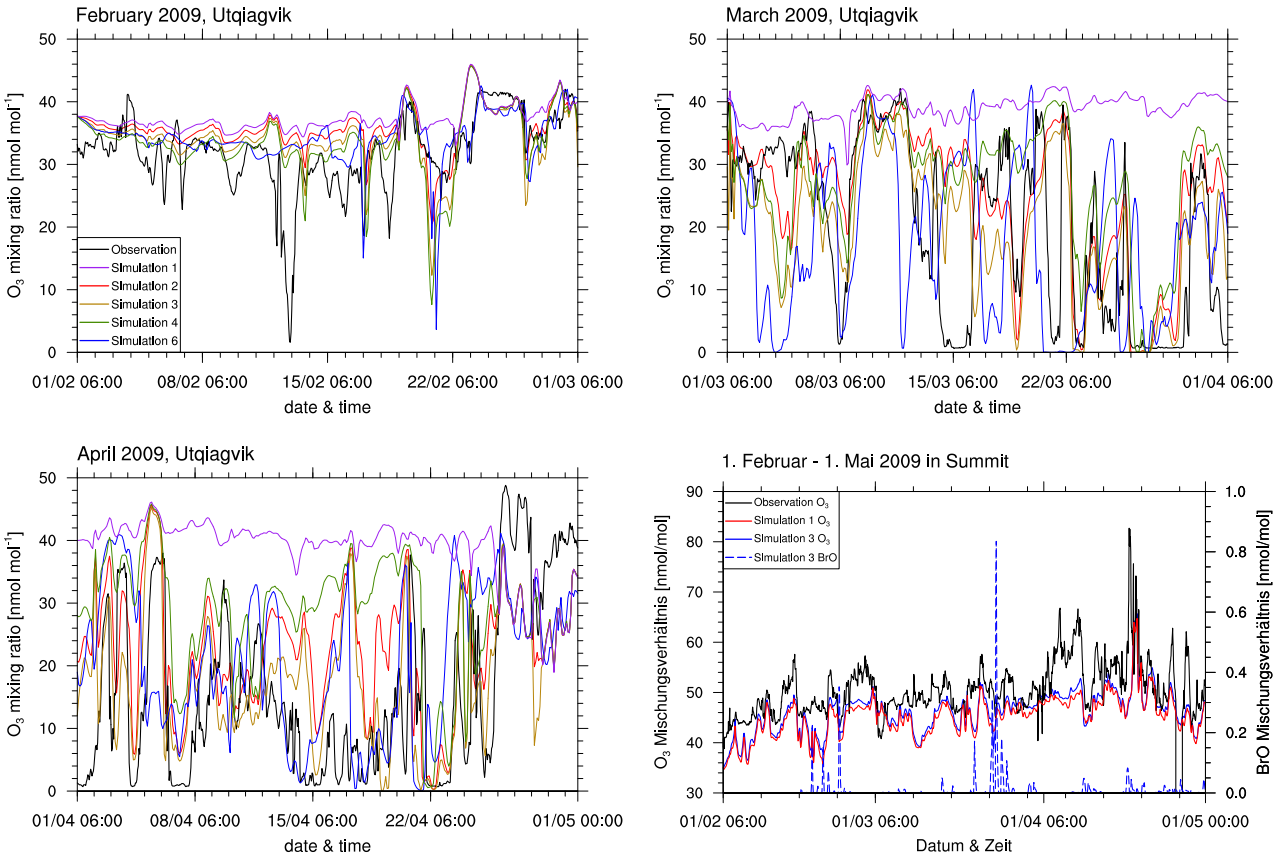

Figure S1. Ozone mixing ratios at Utqiaġvik and at Summit and BrO mixing ratio at Summit. The legend is the same for the first three panels.

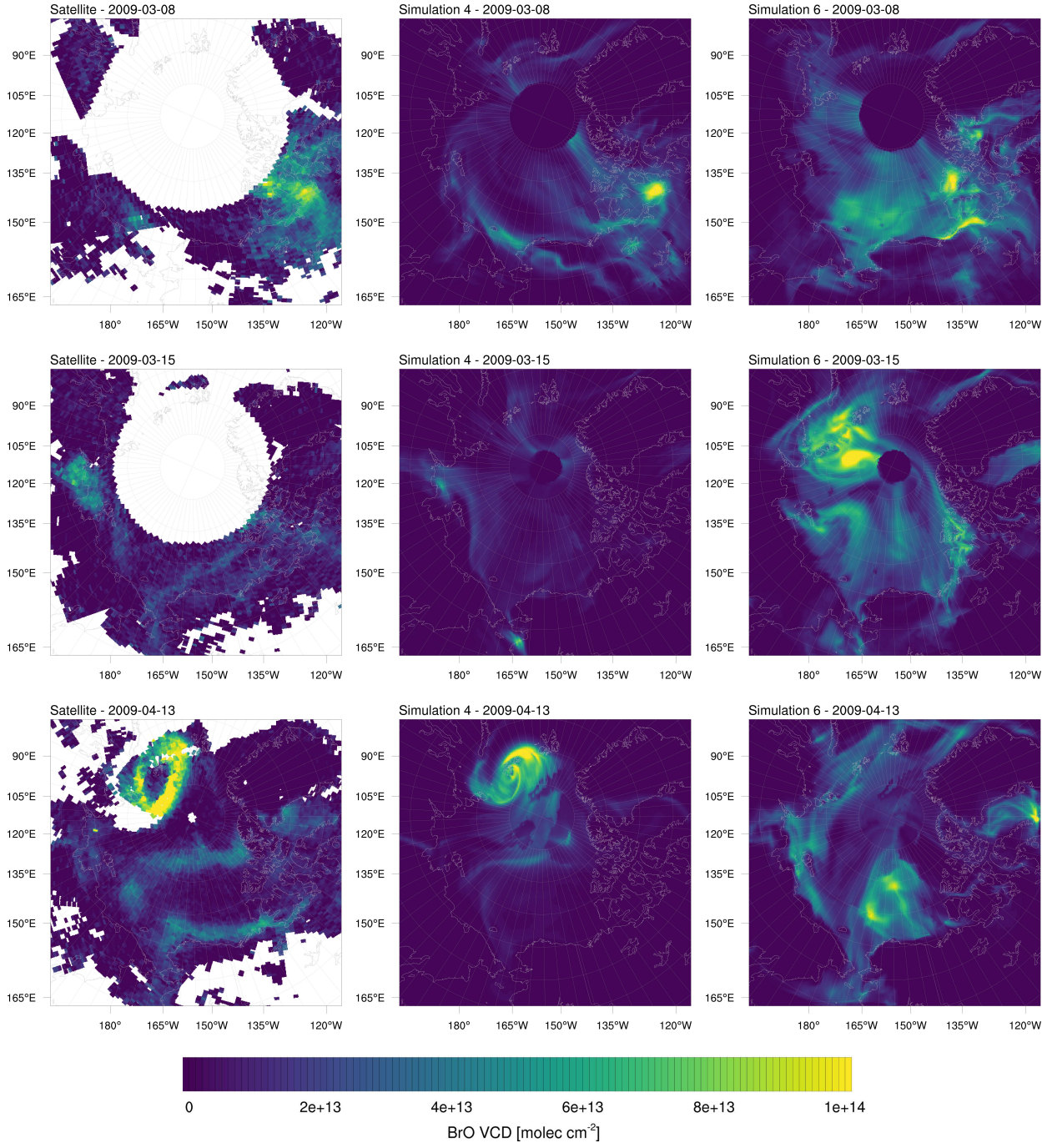

Figure S2. BrO VCDs on selected days in the year 2009. Left: Satellite measurements. Center: Simulation 4 ($\beta = 2$, no bromide oxidation due to ozone). Right: Simulation 6 ($\beta = 1.5$, no nudging).

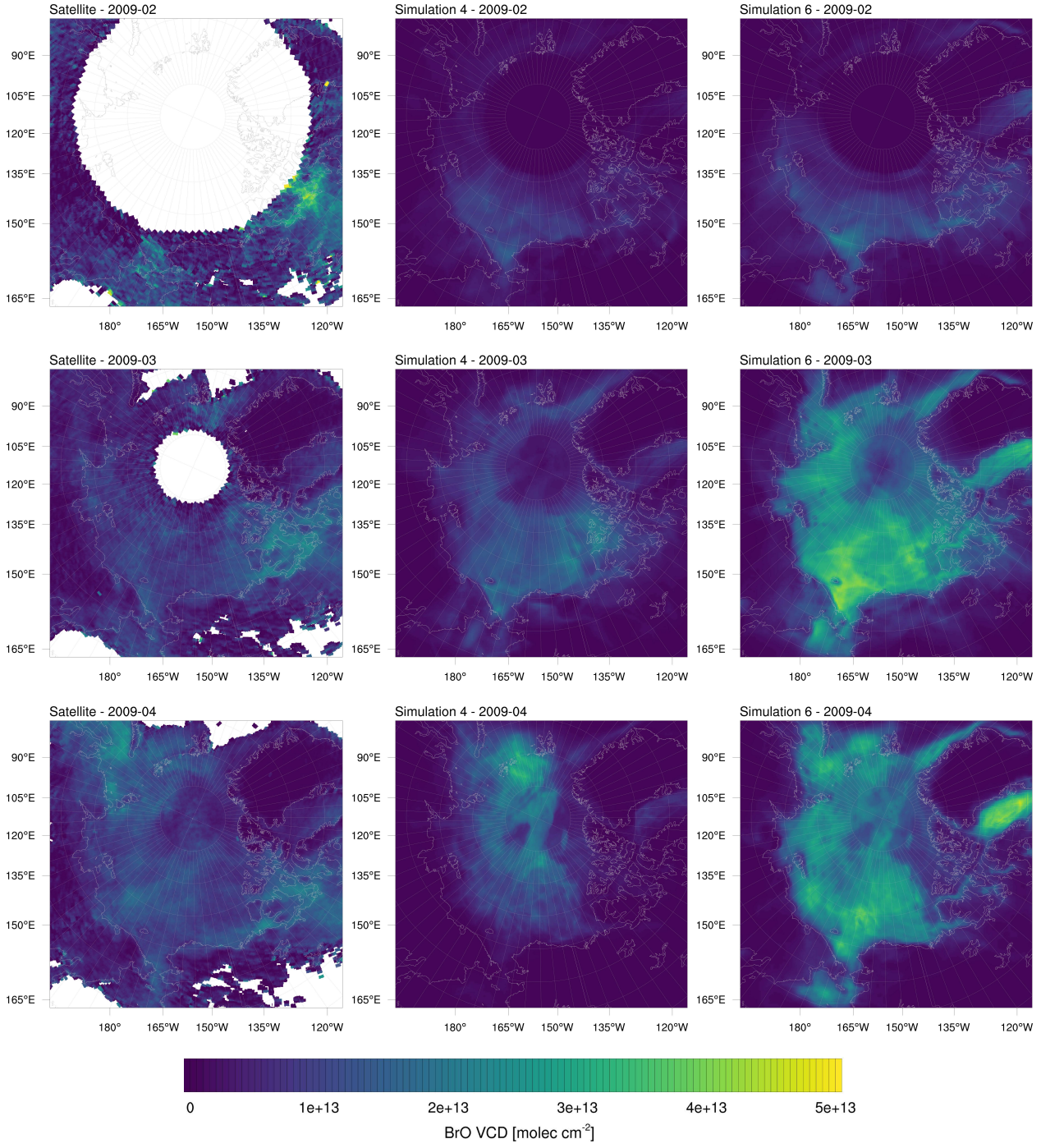

Figure S3. BrO VCDs in the year 2009 averaged over one month. Left: Satellite measurements. Center: Simulation 4 ($\beta = 2$, no bromide oxidation due to ozone). Right: Simulation 6 ($\beta = 1.5$, no nudging).

S5 Vertical BrO at Utqiaġvik

Figure S4 shows modeled vertical BrO profiles convoluted with the MAX-DOAS averaging kernel from March 28, 2009 to April 16, 2009 at Utqiaġvik in comparison to BrO measured with a MAX-DOAS instrument (Frieß et al., 2011). In section 4.2 of the main paper, corresponding profiles for March 28, 2009 to April 16, 2009 are shown and discussed.

S6 N_2O_5 mixing ratio

$BrNO_2$ is photolyzed under sunlight into Br and NO_2. The mixing ratio of N_2O_5 in the lowest grid cell averaged over one month is shown in Fig. S5 for February, March, and April 2009. Large concentrations of N_2O_5 mostly occur in February. Near North Alaska, N_2O_5 is produced by anthropogenic emissions at Prudhoe Bay as predicted by the EDGAR-HTAP anthropogenic emission dataset. N_2O_5 over the Arctic Archipelago is produced by anthropogenic emissions over Baffin Island. N_2O_5 over Siberia is partially produced by anthropogenic emissions resolved by the model, but mostly advected from the boundary conditions. In February, N_2O_5 is very stable due to a lack of sunlight and low temperatures, which explains the large concentrations and decrease in the following months. Since most of the bromine is produced in March and April over FY ice, bromine production due to N_2O_5 has little relevance for the second half of the simulation, but is relevant for the end of February and early March. Bromine emissions due to N_2O_5 in February are unlikely to start a bromine explosion due to the lack of sunlight in the northern regions. However, McNamara et al. (2019) measured N_2O_5 near Utqiaġvik and found 50 pmol mol^{-1} of N_2O_5 for one day in mid March and between 0-15 pmol mol^{-1} otherwise from March to April. Figure S6 shows modeled N_2O_5 in March and April at Utqiaġvik. Most of the time, the N_2O_5 mixing ratio is between 0 and 15 pmol mol^{-1}, but at a few days, more than 50 pmol mol^{-1} of N_2O_5 is predicted. On March 8, a mixing ratio of approximately 300 pmol mol^{-1} is found by the model. All of the events with enhanced mixing ratios of N_2O_5 are caused by advection of polluted air from Prudhoe Bay to Utqiaġvik.

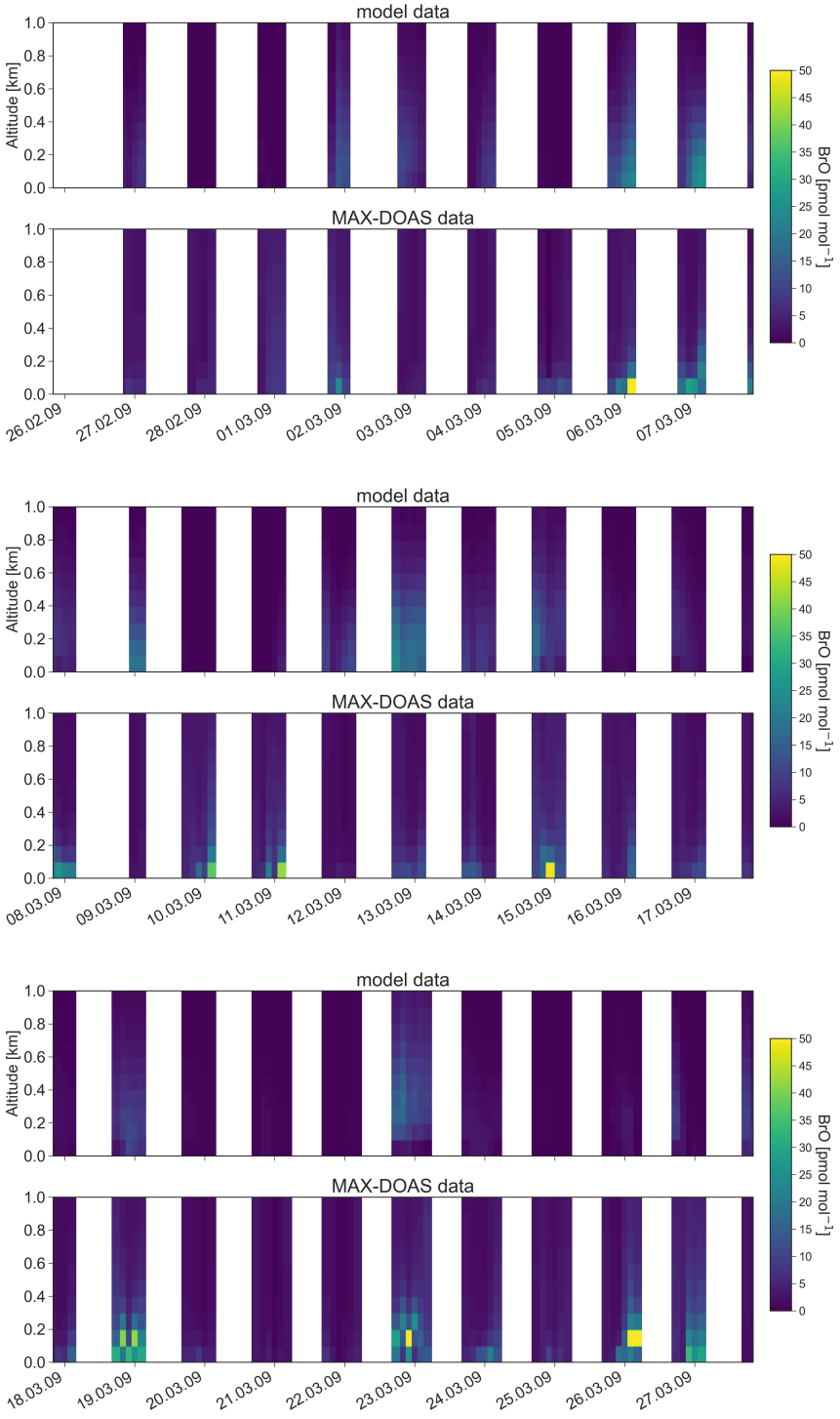

Figure S4. Vertical profiles of BrO from February 26, 2009 to March 27, 2009 at Utqiaġvik. Top: Modeled BrO convoluted with the Max-DOAS averaging kernel, Bottom: BrO observed with Max-DOAS.

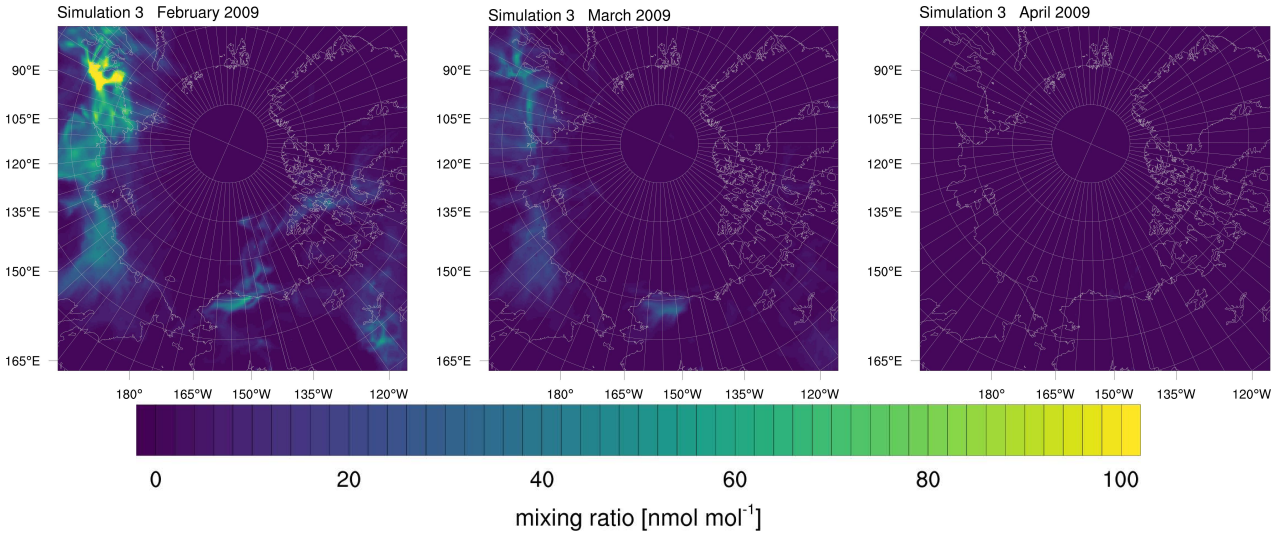

Figure S5. Mixing ratio of N_2O_5 in the lowest grid cell, averaged over one month for February (left), March (center) and April (right).

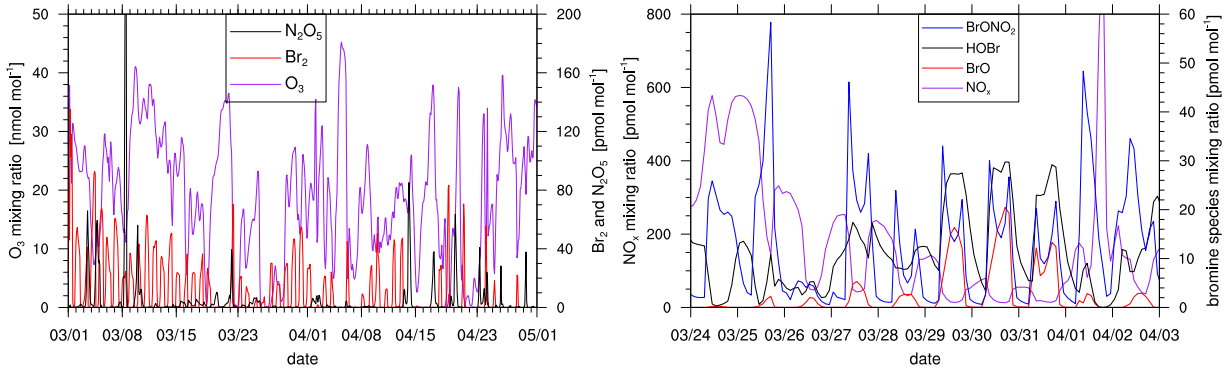

Figure S6. Left: Mixing ratio of ozone, Br_2, and N_2O_5 at Utqiaġvik for simulation 3. Right: Modeled NO_x, BrO, HOBr and $BrONO_2$ at Utqiaġvik for simulation 3. The date shown is for 00:00, GMT-9 (local time at Utqiaġvik, GMT-9). The time range and timezone is chosen to be directly comparable to Figure 7 of Custard et al. (2015).

References

Atkinson, R., Baulch, D. L., Cox, R. A., Crowley, J. N., Hampson, R. F., Hynes, R. G., Jenkin, M. E., Rossi, M. J., Troe, J., and Subcommittee, I.: Evaluated kinetic and photochemical data for atmospheric chemistry: Volume II ; gas phase reactions of organic species, Atmospheric Chemistry and Physics, 6, 3625–4055, https://doi.org/10.5194/acp-6-3625-2006, https://www.atmos-chem-phys.net/6/3625/2006/, 2006.

Atkinson, R., Baulch, D. L., Cox, R. A., Crowley, J. N., Hampson, R. F., Hynes, R. G., Jenkin, M. E., Rossi, M. J., and Troe, J.: Evaluated kinetic and photochemical data for atmospheric chemistry: Volume III - gas phase reactions of inorganic halogens, Atmospheric Chemistry and Physics, 7, 981–1191, https://doi.org/10.5194/acp-7-981-2007, https://www.atmos-chem-phys.net/7/981/2007/, 2007.

Barnes, I., Becker, K. H., and Overath, R. D.: Oxidation of Organic Sulfur Compounds, in: The Tropospheric Chemistry of Ozone in the Polar Regions, edited by Niki, H. and Becker, K. H., pp. 371–383, Springer Berlin Heidelberg, Berlin, Heidelberg, 1993.

Borken, J.: Ozonabbau durch Halogene in der arktischen Grenzschicht, Master's thesis, Heidelberg University, Germany, in German, 1996.

Custard, K. D., Thompson, C. R., Pratt, K. A., Shepson, P. B., Liao, J., Huey, L. G., Orlando, J. J., Weinheimer, A. J., Apel, E., Hall, S. R., Flocke, F., Mauldin, L., Hornbrook, R. S., Pöhler, D., General, S., Zielcke, J., Simpson, W. R., Platt, U., Fried, A., Weibring, P., Sive, B. C., Ullmann, K., Cantrell, C., Knapp, D. J., and Montzka, D. D.: The NO_x dependence of bromine chemistry in the Arctic atmospheric boundary layer, Atmospheric Chemistry and Physics, 15, 10 799–10 809, https://doi.org/10.5194/acp-15-10799-2015, https://acp.copernicus.org/articles/15/10799/2015/, 2015.

DeMore, W. B., Sander, S. P., Golden, D., Hampson, R., Kurylo, M. J., Howard, C. J., Ravishankara, A., Kolb, C., and Molina, M.: Chemical Kinetics and Photochemical Data for Use in Stratospheric Modeling. Evaluation No. 12, Tech. rep., Jet Propulsion Lab., California Inst. of Tech.; Pasadena, CA United Stat, 1997.

Herrmann, M., Cao, L., Sihler, H., Platt, U., and Gutheil, E.: On the contribution of chemical oscillations to ozone depletion events in the polar spring, Atmospheric Chemistry and Physics, 19, 10 161–10 190, https://doi.org/10.5194/acp-19-10161-2019, https://www.atmos-chem-phys.net/19/10161/2019/, 2019.

Madronich, S., Flocke, S., Zeng, J., Petropavlovskikh, I., and Lee-Taylor, J.: Tropospheric Ultraviolet-Visible Model (TUV) version 4.1, National Center for Atmospheric Research, PO Box, 3000, 2002.

McNamara, S. M., Raso, A. R. W., Wang, S., Thanekar, S., Boone, E. J., Kolesar, K. R., Peterson, P. K., Simpson, W. R., Fuentes, J. D., Shepson, P. B., and Pratt, K. A.: Springtime Nitrogen Oxide-Influenced Chlorine Chemistry in the Coastal Arctic, Environmental Science & Technology, 53, 8057–8067, https://doi.org/10.1021/acs.est.9b01797, https://doi.org/10.1021/acs.est.9b01797, pMID: 31184868, 2019.

Nesbitt, F., Monks, P., Payne, W., Stief, L., and Toumi, R.: The reaction O (^{3}P)+ HOBr: Temperature dependence of the rate constant and importance of the reaction as an HOBr stratospheric loss process, Geophysical research letters, 22, 827–830, 1995.

Sander, R. and Crutzen, P. J.: Model study indicating halogen activation and ozone destruction in polluted air masses transported to the sea, Journal of Geophysical Research: Atmospheres, 101, 9121–9138, 1996.

Sander, R., Vogt, R., Harris, G. W., and Crutzen, P. J.: Modelling the chemistry of ozone, halogen compounds, and hydrocarbons in the arctic troposphere during spring, Tellus B: Chemical and Physical Meteorology, 45, 522–532, https://doi.org/10.3402/tellusb.v45i5.16001, https://doi.org/10.3402/tellusb.v45i5.16001, 1997.

Toyota, K., McConnell, J. C., Staebler, R. M., and Dastoor, A. P.: Air–snowpack exchange of bromine, ozone and mercury in the springtime Arctic simulated by the 1-D model PHANTAS - Part 1: In-snow bromine activation and its impact on ozone, Atmospheric Chemistry and Physics, 14, 4101–4133, https://doi.org/10.5194/acp-14-4101-2014, https://www.atmos-chem-phys.net/14/4101/2014/, 2014.

Troe, J.: Predictive possibilities of unimolecular rate theory, Journal of Physical Chemistry, 83, 114–126, 1979.

Wesely, M.: Parameterization of surface resistances to gaseous dry deposition in regional-scale numerical models, Atmospheric Environment (1967), 23, 1293–1304, 1989.